Journal of proteome research

Article

pubs.acs.org/jpr

^{1}H NMR Metabolic Profiling of Earthworm (*Eisenia fetida*) Coelomic Fluid, Coelomocytes, and Tissue: Identification of a New Metabolite—Malylglutamate

Corey M. Griffith,[†] Preston B. Williams,[‡] Luzineide W. Tinoco,[‡,§|] Meredith M. Dinges,[‡] Yinsheng Wang,[†,‡] and Cynthia K. Larive*[,†,‡]

[†]Environmental Toxicology Graduate Program, University of California, Riverside, California 92521, United States

[‡]Department of Chemistry, University of California, Riverside, California 92521, United States

[§|]Laboratório Multiusuário de Análises por Ressonância Magnética Nuclear, Instituto de Pesquisas de Produtos Naturais, Centro de Ciências da Saúde, Universidade Federal do Rio de Janeiro, Rio de Janeiro, Rio de Janeiro CEP 21941-902, Brazil

Supporting Information

ABSTRACT: Earthworm metabolism is recognized as a useful tool for monitoring environmental insults and measuring ecotoxicity, yet extensive earthworm metabolic profiling using ^{1}H nuclear magnetic resonance (NMR) spectroscopy has been limited in scope. This study aims to expand the embedded metabolic material in earthworm coelomic fluid, coelomocytes, and tissue to aid systems toxicology research. Fifty-nine metabolites within *Eisenia fetida* were identified, with 47 detected in coelomic fluid, 41 in coelomocytes, and 54 in whole-worm samples and tissue extracts. The newly detected but known metabolites 2-aminobutyrate, nicotinurate, *Nδ*,*Nδ*,*Nδ*-trimethylornithine, and trigonelline are reported along with a novel compound, malylglutamate, elucidated using 2D NMR and high-resolution MS/MS. We postulate that malylglutamate acts as a glutamate/malate store, chelator, and anionic osmolyte and helps to provide electrolyte balance.

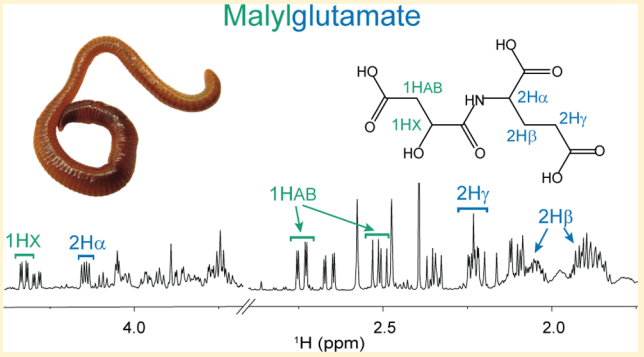

KEYWORDS: *earthworm, coelomic fluid, coelomocytes, metabolomics, NMR spectroscopy, structural elucidation, high-resolution MS/MS, malylglutamate*

INTRODUCTION

As detritivores and ecological engineers, earthworms are at the forefront of soil health and an obvious choice for environmental monitoring. Studies to assess the impacts of heavy metals, persistent contaminants, and pesticides provide evidence of the potential of using earthworm metabolomics as an indicator of ecological stress.[1] Proteomic and transcriptomic strategies have also been assessed as potential methods to monitor earthworm health.[2] Metabolomic and proteomic approaches were used to examine the systemic impact of polybrominated diphenyl ether 47 (PBDE 47) on *Eisenia fetida*.[3] Evidence of perturbation of energy metabolism was observed in both data sets as a result of exposure to PBDE 47, while metabolomics also indicated disruption in osmoregulation and the proteomics results identified changes consistent with oxidative stress, apoptosis, and impeded protein synthesis. In a study of copper toxicity on *Lumbricus rubellus*, disruption of carbohydrate metabolism was observed in the transcriptomics and metabolomics profiling data.[4] These studies highlight the potential of systems biology approaches, including metabolomics and metabolic profiling, to interpret the biochemical changes resulting from environmental insults and motivate our efforts to seek a more comprehensive analysis of the *E. fetida* metabolome.

Metabolic studies have largely focused on whole-worm extracts but have also been extended to coelomic fluid (CF), a yellow liquid that fills the worm's coelom that connects to the environment through a dorsal pore in each of its segments.[1,5] Despite these pores, the earthworm's coelom avoids sepsis, leading many researchers to hunt for unique defense proteins and peptides within the CF and to better understand the role of coelomocytes (CC) in combating pathogens and parasites.[6] CF holds cytotoxic, hemolytic, proteolytic, and antimicrobial defense mechanisms and plays critical roles in immunity, movement, excretion, nutrient storage, and metabolism.

In assessing the effects of exposure to a contaminant, CF offers several advantages over whole-worm extracts including nonlethal sampling, simple sample preparation, and greater temporal resolution.[7] Although typically discarded for metabolomic studies, CC are free-moving cells within the CF that

Received: June 22, 2017
Published: July 28, 2017

DOI: 10.1021/acs.jproteome.7b00439
J. Proteome Res. 2017, 16, 3407−3418

serve immunological and hepatocytic functions. To our knowledge, the CC metabolome has not been profiled or used in metabolomic studies, although it has been used to assess toxicity. For example, Burch et al. described an in vitro CC immunotoxicity assay, while others have used the comet and other genotoxic assays to evaluate genotoxicity.[8,9] Therefore, analysis of earthworm CC metabolites may provide an additional source of information to augment these toxicity assessments.

From relatively inert soil amendments like sulfur and lime to the transport of agricultural and industrial contaminants to foods, methods to measure and control various aspects of ecological stress are essential for crop production, water quality, and environmental health.[10,11] Upon exposure to 3-fluoro-4-nitrophenol, Bundy et al. demonstrated that relative concentrations of trimethylamine *N*-oxide and succinate increased in the CF of *E. veneta*, while malonate and acetate concentrations decreased. The metabolomic impact of endosulfan on the CF and whole-tissue extract of *E. fetida* was measured via the Organization for Economic Co-operation and Development (OECD) filter paper test.[12] Decreases in α-ketoglutarate, malate, spermidine, and succinate were observed in the tissue and CF of exposed worms, while alanine, ATP, betaine, lactate, and *myo*-inositol levels increased. In the whole-worm extract, fumarate also decreased in comparison with the control. Similar metabolic perturbations were found in further studies on endosulfan and endosulfan sulfate in soil.[13] Additionally, CF and whole-worm metabolomics has been used to distinguish between earthworm species, including the morphologically similar *E. fetida* and *E. andrei*.[14]

The earthworm's habitat has evolved its unique metabolome to help it adapt to changing water content and temperatures, complex food sources, and soil types. This work aims to provide a more complete metabolic profile, advancing our understanding of the biochemical impacts of environmental stress, and ultimately, expanding insights into the differences in metabolism among species. In this work, nuclear magnetic resonance (NMR) spectroscopy was used to profile the *E. fetida* CF and CC metabolomes (i.e., the coelom metabolome) and compare these against extracts of whole-worm and tissue (i.e., worm samples post-CF/CC extrusion) to better understand the biochemical role of the coelom and expand overlooked facets of the earthworm metabolome. NMR is well-suited for metabolomic analyses and environmental research and is independent of solvent choice, polarity, and pK_a. A robust analytical tool, NMR offers a large dynamic range and is inherently quantitative, in that peak intensity is directly proportional to concentration.[15−17]

EXPERIMENTAL PROCEDURES

Earthworm Culturing

Earthworms (*Eisenia fetida*) were purchased from Ward's Science (Rochester, NY) and cultured in Magic Worm Ranches containing Magic Worm bedding (Magic Products, Amherst Junction, WI).[18] Earthworms were fed biweekly with Magic Worm food, and bedding was changed every 4 months to maintain colony health. Bedding was prepared by adding 4 L of dechlorinated water for every bag of bedding and then left for 24 h prior to transferring the earthworms. Earthworms from different ranches were mixed together when changing soils to main population homogeneity. Only adult earthworms with fully developed clitellia were used for this study.

Coelomic Fluid Extrusion

CF was extruded from the earthworms similarly to previously described methods.[7,12] Earthworms were dipped in EMD Millipore Simplicity ultrapure water to remove soil and patted dry. The earthworm was transferred to a 35 × 10 mm Falcon Petri dish containing 500 μL of 0.1% NaCl in ultrapure water. A voltage was applied across the earthworm 10 times in <1 s increments using a 9 V battery with a wire snap. For pooled samples, this step is repeated with additional worms. Next, the fluid was transferred to a 1.5 mL Eppendorf tube, and the Petri dish was rinsed with 500 μL of NaCl solution and transferred to the same Eppendorf tube. The sample was centrifuged for 20 min at 16 168*g*, and the supernatant evaporated overnight using a Savant SC110 Speedvac equipped with a refrigerator vapor trap (RVT400). The dried samples were stored at −80 °C until analysis.

Coelomocyte Extraction

Following centrifugation and transfer of CF, a pellet of CC and biosolids remains. Cellular metabolism was quenched by adding 500 μL of ice-cold Fischer Scientific Optima methanol (Fair Lawn, NJ) to the pellet immediately after CF transfer. The sample was vortexed and sonicated briefly and stored on ice until extraction. An equal quantity of ice-cold ultrapure water was added to the sample and mixed using vortex and sonication. Lipids were removed with two additions of 250 μL of ice-cold chloroform (Macron Fine Chemical, Center Valley, PA). The aqueous layer was transferred to a fresh tube, dried via Speedvac, and stored at −80 °C.

Whole-Worm and Tissue Extraction

Metabolites were extracted from earthworms after CF/CC extrusion, referred to here as tissue extracts, and whole-worm or whole organism extracts, as typically reported in literature. Earthworms were flash-frozen in liquid nitrogen, lyophilized, and homogenized by bead-beating with 1 mL of (50:50) cold methanol/water. The sample was centrifuged at 16 168*g* for 20 min, and the supernatant was transferred to a new tube for cleanup with 500 μL of ice-cold chloroform. The aqueous layer was dried and stored at −80 °C.

Weak Cation Exchange Separation

A dried 10-worm pooled CF sample was reconstituted in 2 mL of ultrapure water and titrated to pH 3 with hydrochloric acid (Fisher Scientific) prior to separation on a PerkinElmer Supra-Clean SPE WCX column (100 mg/3 mL) (France). The cartridge was conditioned with 6 mL of methanol and ultrapure water, loaded, and washed with 1 mL of methanol until dry. Cations were eluted with 2 mL of 84:14:2 Fischer Scientific Optima acetonitrile/H_2O/trifluoroacetic acid (Acros, Fair Lawn, NJ).

NMR Sample Preparation

Most samples for NMR analysis were reconstituted with 500 μL of 50 mM phosphate buffer in D_2O (pD 7.45) containing 0.5 mM 3-(trimethylsilyl)propane-1-sulfonic acid-d_6 (DSS-d_6) and 0.2 mM ethylenediaminetetraacetic acid-d_{16} (EDTA-d_{16}) (Cambridge Isotope Laboratories, Tewksbury, MA) and vortexed until dissolved. For experiments conducted in 90% H_2O, samples were reconstituted in 500 μL of ultrapure water and vortexed until dissolved. The samples were passed through a washed 3K Amicon Ultra 0.5 mL centrifugal filter to remove macromolecules. Centrifugal filters were washed to remove glycerol by mixing on a stir plate for ∼20 h in 400 mL of ultrapure water, with the water replaced after ∼5 h. Prior to use,

DOI: 10.1021/acs.jproteome.7b00439
J. Proteome Res. 2017, 16, 3407−3418

Table 1. List of Aqueous Metabolites and Their ^{1}H Chemical Shifts Detected in Pooled and Individual Coelomic Fluid (CF), Coelomocytes (CC), and Tissue Extracts[a]

no.	metabolite	coelomic fluid	coelomocytes	tissue	^{1}H chemical shifts (ppm)[b]
1	acetate	a,b,e	a,b	a,b,e	1.91 (s)
2	adenosine diphosphate		a,b,c,d	a,b,c,d	4.22 (m), 4.38 (m), 4.53 (t), 6.14 (d), 8.25 (s), 8.52 (s)
3	adenosine monophosphate		a,b,c,d	a,b,c,d	4.01 (dd), 4.36 (dd), 4.50 (dd), 6.13 (d), 8.25 (s), 8.60 (s)
4	adenosine triphosphate		a,b,c,d	a,b,c,d	4.22 (m), 4.38 (m), 4.53 (t), 6.14 (d), 8.25 (s), 8.52 (s)
5	alanine	a,b,c,d,e	a,b,c,d,e	a,b,c,d,e	1.47 (d), 3.78 (q)
6	asparagine	a,b,c,d		a,b,c,d	2.91 (m), 4.01 (dd)
7	aspartate	a,b,c,d	a,b,c,d	a,b,c,d,e	2.74 (m), 3.89 (dd)
8	betaine	a,b,c,d,e	a,b,c,d,e	a,b,c,d,e	3.26 (s), 3.90 (s)
9	choline	a,b,c,d,e	a,b,c,d,e	a,b,c,d,e	3.21 (s), 3.52 (m), 4.07 (m)
10	cytosine	a,b,c,d			5.95 (d), 7.49 (d)
11	formate	a,b,e	a,b	a,b,e	8.44 (s)
12	fumarate	a,b,e	a,b,e	a,b,e	6.50 (s)
13	glucose	a,b,c,d,e	a,b,c,d,e	a,b,c,d,e	3.23 (dd), 3.39 (m), 3.46 (m), 3.52 (dd), 3.73 (m), 3.82 (m), 4.83 (d), 5.22 (d)
14	glutamate	a,b,c,d,e	a,b,c,d,e	a,b,c,d,e	2.05 (m), 2.12 (m), 2.34 (m), 3.74 (q)
15	glutamine	a,b,c,d,e	a,b,c,d,e	a,b,c,d	2.02 (m), 2.12 (m), 3.76 (t)
16	glycine	a,b,c,d	a,b,c,d,e	a,b,c,d,e	3.54 (s)
17	glycerol			a,b,c,d,e	3.60 (m), 3.77 (m)
18	glycerophosphocholine	a,b,e	a,b,e	a,b,e	3.22 (s), 3.64 (m), 3.91 (m), 4.32 (m)
19	histidine	a,b,c,d		a,b,c,d	3.13 (dd), 2.23 (dd), 3.97 (dd), 7.06 (d), 7.80 (d)
20	histidine-betaine	a,b,e	a,b,e	a,e	3.26 (s)
21	inosine	a,b,c,d	a,b,c,d	a,b,c,d	3.83 (dd), 3.91 (dd), 4.27 (dd), 4.43 (dd), 6.09 (d), 8.23 (s), 8.33 (s)
22	isoleucine	a,b,c,d	a,b,c,d	a,b,c,d,e	0.93 (t), 1.00 (d), 1.25 (m), 1.46 (m), 1.97 (m), 3.66 (d)
23	lactate	a,b,c,d,e	a,b,c,d,e	a,b,c,d,e	1.32 (d), 4.10 (q)
24	leucine	a,b,c,d	a,b,c,d	a,b,c,d,e	0.95 (t), 1.71 (m), 3.72 (m)
25	lysine			a,b,c,d,e	1.47 (m), 1.72 (m), 1.90 (m), 3.02 (t), 3.74 (t)
26	malate	a,b,c,d,e	a,b,c,d,e	a,b,c,d,e	2.36 (dd), 2.66 (dd), 4.29 (dd)
27	**malylglutamate***	**a,b,c,d,e**	**a,b,c,d,e**	**a,b,c,d,e**	**1.88 (m), 2.05 (m), 2.23 (m), 4.14 (dd), 2.52 (dd), 2.74 (dd), 4.33 (dd)**
28	maltose-x	a,b,c,d,e	a,b,c,d,e	a,b,c,d,e	3.27 (dd), 3.41 (t), 3.58 (m), 3.63 (m), 3.66 (m), 3.70 (m), 3.76 (m), 3.84 (m), 3.90 (dd), 3.93 (d), 3.96 (m), 5.22 (d), 5.40 (d)
29	mannose			a,b,c,d	3.37 (ddd), 3.56 (t), 3.65 (m), 3.74 (m), 3.80 (m), 3.84 (m), 3.88 (dd), 3.93 (m), 5.17 (m)
30	*myo*-inositol	a,b,c,d,e	a,b,c,d,e	a,b,c,d,e	2.67 (t), 3.52 (dd), 3.61 (t), 4.05 (t)
31	nicotinamide			a,b,c,d	7.57 (m), 8.22 (m), 8.69 (dd), 8.90 (dd)
32	nicotinate			a,b,c,d	7.51 (dd), 8.24 (m), 8.60 (dd), 8.93 (d)
33	**nicotinurate**			**a,b,c,d**	**3.96 (s), 7.57 (m), 8.23 (tt), 8.68 (dd), 8.91 (m)**
34	*N*,*N*-dimethylhistidine	a,b,c,d	a,b,c,d	a,b,c,d	2.90 (s), 3.25 (dd), 3.86 (dd), 7.04 (s), 7.76 (s)
35	*Nε*,*Nε*,*Nε*-trimethyllysine	a,b,c,d,e	a,b,c,d,e	a,b,c,d,e	1.46 (m), 1.89 (m), 3.11 (s), 3.34 (m), 3.75 (t)
36	***Nδ*,*Nδ*,*Nδ*-trimethylornithine***	**a,b,c,d,e**	**a,b,c,d,e**	**a,b,c,d,e**	**1.94 (m), 3.13 (s), 3.38 (m), 3.78 (t)**
37	*N*,*N*,*N*-trimethyltaurine*	a,b,e	a,b,e	a,b,e	3.19 (s)
38	phenylalanine	a,b,c,d		a,b,c,d,e	3.20 (m), 3.98 (dd), 7.32 (d), 7.36 (m), 7.42 (m)
39	proline-betaine			a,b,e	3.10 (s), 3.29 (s)
40	propionate	a,b,c,d		a,b,c,d	1.05 (t), 2.17 (m)
41	putrescine	a,b,c,d,e	a,b,c,d,e	a,b,c,d,e	1.76 (m), 3.05 (m)
42	pyruvate	a,b,e	a,b,e	a,b,e	2.35 (s)
43	riboflavin	a,b,c,d,e	a,b,c,d,e	a,b,c,d	2.47 (s), 2.58 (s), 3.72 (dd), 3.87 (dd), 3.92 (m), 3.97 (m), 4.43 (m), 4.95 (m), 5.13 (m), 7.95 (s), 7.97 (s)
44	*scyllo*-inositol	a,b,e	a,b,e	a,b,e	3.33 (s)
45	spermidine	a,b,c,d,e	a,b,c,d,e	a,b,c,d,e	1.78 (m), 2.11 (m), 3.08 (m)
46	spermine	a,b,c,d,e	a,b,c,d,e	a,b,c,d,e	1.82 (m), 2.12 (m), 3.11 (m)
47	succinate	a,b,e	a,b,e	a,b,e	2.40 (s)
48	threonine	a,b,c,d	a,b,c,d,e	a,b,c,d,e	1.32 (d), 3.57 (d), 4.24 (m)
49	trehalose	a,b,c,d	a,b,c,d	a,b,c,d	3.44 (t), 3.64 (dd), 3.76 (m), 3.81 (m), 5.18 (d)
50	**trigonelline**			**a,b,c,d**	**4.43 (s), 8.08 (m), 8.83 (m), 9.11 (s)**
51	tyrosine	a,b,c,d		a,b,c,d,e	3.05 (dd), 3.19 (dd), 3.93 (dd), 6.89 (m), 7.18 (m)
52	uridine 5′-diphospho-*N*-acetylglucosamine	a,b,c,d	a,b,c,d	a,b,c,d	2.07 (s), 3.55 (dd), 3.80 (m), 3.86 (dd), 3.92 (dd), 3.98 (tt), 4.21 (m), 4.28 (m), 4.36 (m), 5.51 (dd), 3.96 (d), 5.97 (d), 7.95 (d)
53	uridine	a,b,c,d			3.79 (dd), 3.90 (dd), 4.12 (m), 4.22 (dd), 4.34 (dd), 5.89 (d), 5.91 (d), 7.86 (d)
54	valine	a,b,c,d	a,b,c,d	a,b,c,d,e	0.98 (d), 1.03 (d), 2.27 (m), 3.60 (d)
55	α-ketoglutarate	a,b,c,d,e	a,b,c,d	a,b,c,d	2.43 (t), 3.00 (t)
56	γ-butyrobetaine	a	a		3.02 (m), 2.26 (t), 3.12 (s), 3.31 (m)

DOI: 10.1021/acs.jproteome.7b00439
J. Proteome Res. 2017, 16, 3407−3418

Table 1. continued

no.	metabolite	coelomic fluid	coelomocytes	tissue	^{1}H chemical shifts (ppm)[b]
57	**2-aminobutyrate**	**a,b,c,d**			**0.97 (t), 1.89 (m), 3.70 (t)**
58	2-hexyl-5-ethyl-furan-3-sulfonate (HEFS)*			a,b,c,d,e	0.84 (t), 1.17 (t), 1.28 (m), 1.63 (m), 2.58 (q), 2.82 (t), 6.17 (s)
59	3-hydroxybutyrate	a,b,c,d			1.18 (d), 2.29 (m), 2.39 (m), 4.13 (m)

[a]NMR spectra in which metabolites are confirmed are noted (a = 1D ^{1}H NMR, b = 2D ^{1}H *J*-Resolved, c = COSY, d = TOCSY, and e = ^{1}H−^{13}C HSQC) within each matrix. Bolded metabolites are new to earthworm metabolomics, and the spectra of authentic standards were not recorded for metabolites marked with an *. [b]Signal multiplicity is represented by s = singlet, d = doublet, dd = double doublet, m = multiplet, q = quartet, and t = triplet.

the filters were rinsed a final time with 500 μL of D_2O buffer and spun at 16 168*g* for 15 min. Samples were applied to the filter and centrifuged at the same speed for 30 min. A 400 μL aliquot of the filtered extract was transferred to a 5 mm NMR tube with 200 μL of buffer and mixed well prior to analysis. For the 90% H_2O samples, 60 μL of D_2O buffer was added to 400 μL of filtrated and 40 μL of ultrapure water prior to titration with deuterium chloride (Sigma-Aldrich, St. Louis, MO).

NMR Acquisition Parameters

A Bruker Avance NMR spectrometer operating at 599.52 MHz and equipped with a BBI and a Bruker Avance III NMR spectrometer operating at 700.23 MHz and equipped with a TCI CryoProbe were used for these experiments. ^{1}H NMR survey spectra were acquired at 600 MHz using presaturation water suppression (zgpr) with 512 scans, 32 dummy scans, 2 s delay time, 2.38 s acquisition time, 11.4864 ppm spectral width, and 32 768 points at 25 °C. Water suppression was conducted using 1D NOESY (noesypr1d) with presaturation during the 120 ms mixing time for the ^{1}H survey spectra with 700 MHz and were acquired with 256 scans, 16 dummy scans, 2 s delay time, 2.03 s acquisition time, 11.5169 ppm spectra width, and 32 768 points at 25 °C. At 600 MHz, the double quantum filtered COSY spectra (cosygpprqf) were measured with a 45° pulse, while the TOCSY spectra (mlevgpphw5) were measured using a mixing time of 120 ms.[19−22] Both experiments were performed with 32 scans and 16 dummy scans, with 2048 points acquired in F2 and 512 in F1. The 2D *J*-Resolved spectra (jresgpprqf) were acquired at 600 MHz with 8192 points in F2 and 64 in F1 with 64 scans and 16 dummy scans.[23] Lastly, the ^{1}H−^{13}C edited HSQCs (hsqcedetgpsisp2.2) were acquired with 2048 by 128 points in F2 and F1, respectively, at 700 MHz.[24−27]

Data Processing

Bruker TopSpin 3.2 was used for initial phasing and chemical shift referencing to DSS (0 ppm) prior to processing with MestReNova 10. Free induction decays (FIDs) for ^{1}H survey spectra were apodized by multiplication with an exponential function equivalent to 1 Hz line broadening, zero-filled to 131 072 points, drift corrected by 5%, and baseline corrected using Bernstein Polynomial Fit. All 2D spectra were baseline corrected using Bernstein Polynomial Fit with polynomial order 3 and the reduce T_1 noise function was applied. For the TOCSY, COSY, and HSQC, spectra were zero filled to 4096 by 2048 in both dimensions, while the 2D ^{1}H *J*-resolved spectra are zero filled to 16 384 by 128. The TOCSY and HSQC spectra are apodized using a cosine^2 function in both dimensions, while the COSY and 2D ^{1}H *J*-resolved spectra were apodized with a sine^2 function.

Authentic standards were acquired and analyzed for all assigned resonances unless noted with a * in Table 1. The Human Metabolome Database and Madison Metabolomics Consortium Database were used to aid metabolite identification.[28,29]

Sample Preparation for Mass Spectrometry Analysis

A five-worm CF was reconstituted in 1 mL of (50:50) H_2O/methanol with 0.1% formic acid (Sigma-Aldrich), 300 μL was transferred to a fresh tube and diluted to 1 mL with mobile phase. The sample was centrifuged at 16 168*g* for 1 min prior to direct infusion (DI)−MS experiments. Liquid chromatography−mass spectrometry (LC−MS) experiments were conducted using eluate from the WCX separations. WCX eluates were first reconstituted in 100 μL of ultrapure water with 0.1% trifluoracetic acid for desalting with Agilent OMIX SCX 100 μL tips, following the manufacturer's instructions. Desalted samples were dried via Speedvac, reconstituted in 20 μL of 0.1% formic acid in ultrapure water, centrifuged at 16 168*g* for 1 min, and subjected to LC−MS.

Direct Infusion Tandem Mass Spectrometry Analysis

Samples were loaded into a 500 μL syringe and introduced into an LTQ-Orbitrap Velos mass spectrometer equipped with a heated electrospray ionization source (Thermo Fisher Scientific, San Jose, CA) at a flow rate of 10 μL/min.[30] The instrument was operated in the positive-ion mode, and full-scan MS in the range of m/z 50−1000 were acquired in the Orbitrap mass analyzer with the resolution of 100 000 at m/z 400. The precursors for the metabolites of interest were subjected to collision-induced dissociation (CID) to acquire the MS/MS in the linear ion trap.

Liquid Chromatography−Tandem Mass Spectrometry Analysis

Online LC−MS/MS analysis was performed on an LTQ-Orbitrap Velos mass spectrometer coupled to an EASY-nLC 1000 HPLC system and a nanoelectrospray ionization source (Thermo Fisher Scientific, San Jose, CA). Sample injection, enrichment, desalting, and HPLC separation were conducted automatically. The nLC was equipped with an in-house packed trapping column, followed by an in-house packed separation column, both packed with ReproSil-Pur C18-AQ resin (3 μm, Dr. Maisch HPLC, Germany). The metabolites were separated using a 120 min linear gradient of 2−40% acetonitrile in 0.1% formic acid at a flow rate of 230 nL/min and electrosprayed (spray voltage 1.8 kV) into an LTQ-Orbitrap Velos mass spectrometer operated in the positive-ion mode. Full-scan MS (50−1000 m/z) were acquired at a resolution of 60 000 (at m/z 400) and followed by data-dependent acquisition (normalized collision energy of 35.0) of MS/MS for the 20 most abundant ions found in the full-scan MS exceeding a threshold of 1000 counts.

DOI: 10.1021/acs.jproteome.7b00439
J. Proteome Res. 2017, 16, 3407−3418

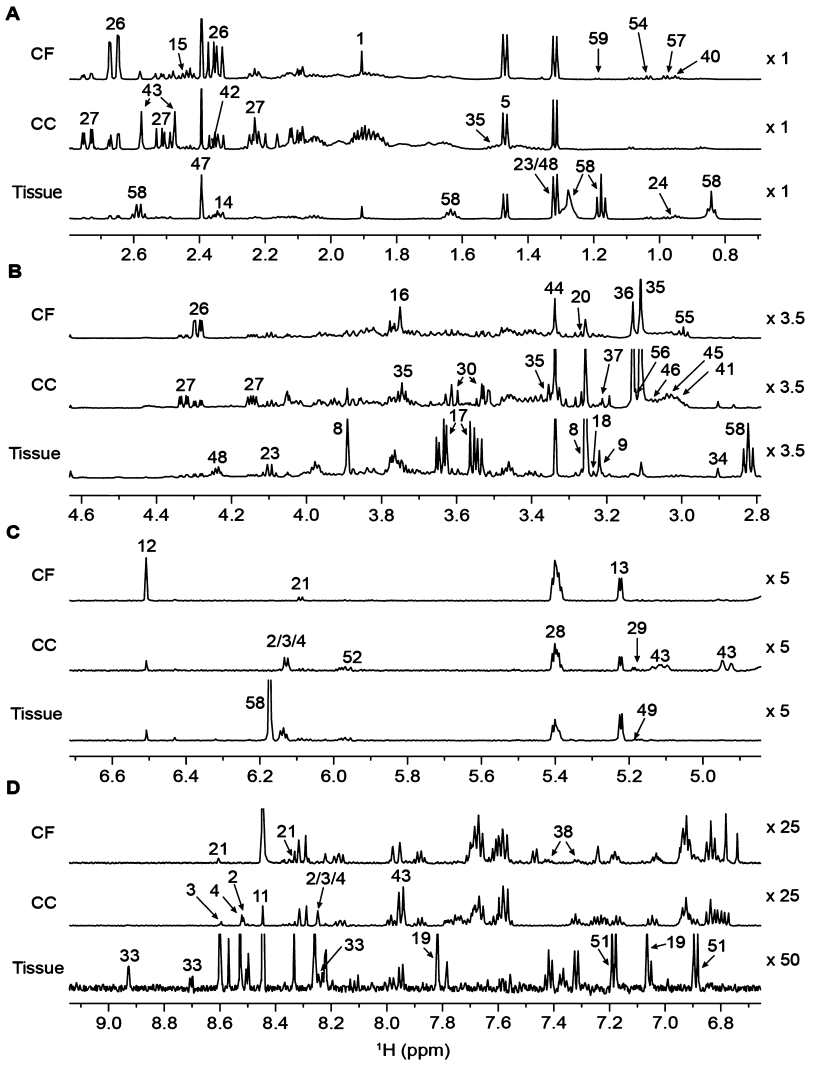

Figure 1. ^{1}H NMR spectra of 20-worm concentrated coelomic fluid (CF), 60-worm concentrated coelomocytes (CC), and 55 mg of pooled tissue extracts. The relative intensity of each region is listed on the right side of each spectrum. The spectra are divided into four regions: (A) 0.75−2.8, (B) 2.8−4.6, (C) 4.7−6.7, and (D) 6.7−9.2 ppm and resonances are annotated to their corresponding metabolite in Table 1. Several metabolites were identified but not annotated due to low intensity or because they were present in only a subset of samples.

Mass Spectrometry Data Analysis

Data were analyzed manually using Xcalibur Qual Browser (Thermo Fisher Scientific) software. Raw MS data were analyzed by searching the calculated exact mass of each metabolite of interest. Using the advanced processing within chromatogram ranges, data were analyzed by enabling smoothing using the boxcar algorithm with seven points, and the mass tolerance was user-defined at 10 ppm. The plot type was set to mass range with the full MS scan filter applied using the MS detector and the ICIS peak algorithm was used. The calculated exact mass of the metabolite of interest was placed in the range and the data were searched for analyte peaks. Each metabolite under investigation was searched individually using the same method. Signal was then averaged in the time range for the peaks found in the ion chromatogram to give MS for each metabolite.

RESULTS

This study aimed to provide a more comprehensive survey of *E. fetida* endogenous metabolites using pooled and individual tissue, CF, and CC samples. ^{1}H NMR spectroscopy (Figure 1) was employed to detect 59 metabolites within *E. fetida*, with 47 detected in CF, 41 in CC extracts, and 54 in extracts of whole-worm samples and tissue samples depleted of CF and CC (referred to as tissue samples). Because of the high similarity between whole-worm and tissue extracts, we will only discuss our tissue data sets and reserve discussion of whole-worm extracts to data sets reported in literature. Five metabolites, 2-aminobutyrate, malylglutamate, nicotinurate, *Nδ,Nδ,Nδ*-trimethylornithine, and trigonelline, are new to earthworm metabolomics (Table 1). Importantly, we believe this to be the first report of the identification of malylglutamate in any biological system.

^{1}H NMR Metabolic Profiling of Earthworm CF, CC, and Tissue

Global metabolic profiling was conducted using an array of NMR experiments to determine endogenous metabolites within earthworm tissue, CF, and CC. These findings are highlighted in the ^{1}H NMR spectra in Figure 1 and are summarized in Table 1 and Table S-1. In cases where it was not possible to conclusively identify metabolite spectroscopic signatures at neutral pH, the titration of a pooled CF sample

DOI: 10.1021/acs.jproteome.7b00439
J. Proteome Res. 2017, 16, 3407−3418

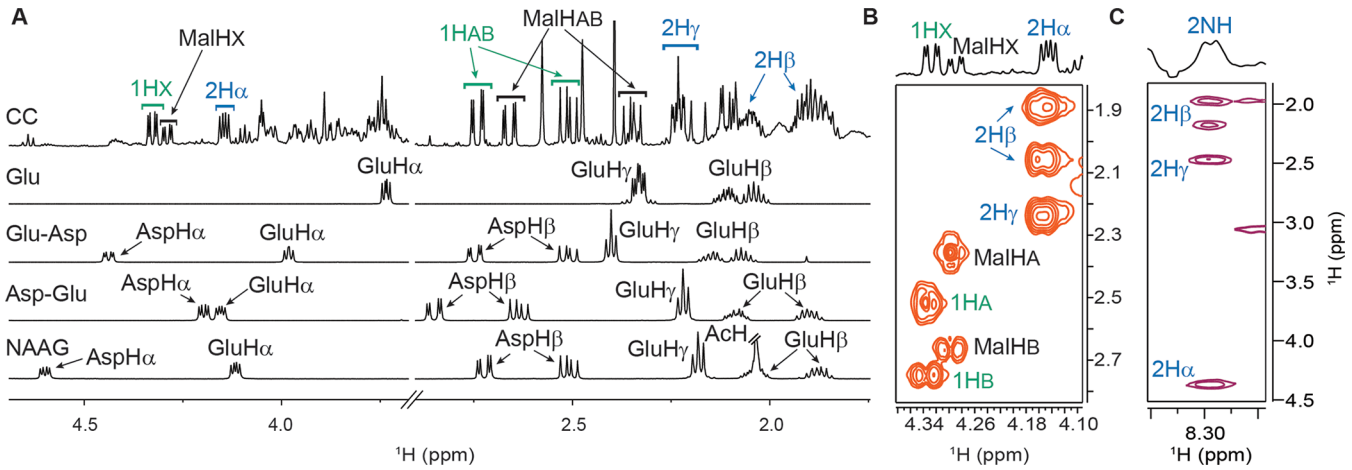

Figure 2. NMR spectra of unassigned resonances and comparison of closely related structures. (A) ^{1}H NMR spectra of CC and the authenticated standards of glutamate (Glu), glutamylaspartate (Glu-Asp), aspartylglutamate (Asp-Glu), and *N*-acetylaspartylglutamate (NAAG) are stacked below and proton position is annotated. The two sets of unassigned resonances are annotated in the CC spectrum as 1H (green) and 2H (blue), and the malate (Mal) resonances are annotated in black. (B) TOCSY spectrum of CC annotated with the correlated spin systems of 1H, 2H, and Mal. (C) TOCSY spectrum of pooled CF sample at pD 3.18 in 90% H_2O, revealing a strong correlation between an amide proton and a spin system resembling glutamate.

in ∼0.5 intervals between pD 3.06 and 7.40 was useful to resolve resonances and confirm assignments (Figure S-1). For instance, the downfield shift of malate reveals the gamma protons of glutamate (2.35 ppm, Figure S-1B) beginning at pD 5.42 and the methyl resonance of threonine at pD 4.06, as lactate shifts downfield with increasing acidity (1.32 ppm, Figure S-1C).

Because of the complexity of the samples, correlation spectroscopy (COSY) and total correlation spectroscopy (TOCSY) were employed to reveal coupled spins and spin systems, assisting in identification of metabolites such as the heavily overlapped polyamines, putrescine, spermidine, and spermine, as annotated in the representative COSY spectrum in Figure S-2.[19−22] Further confidence in resonant assignments was gained using homonuclear 2D *J*-resolved spectroscopy experiments to differentiate several overlapping peaks and was particularly useful for assigning singlets that were filtered out in the double quantum filtered COSY spectra or resonances uncoupled to a spin system in the TOCSY spectra.[23] The 2D ^{1}H *J*-resolved spectra greatly aided identification of the betaine analog singlets between 3.0 and 3.4 ppm (Figure S-3A), including betaine, choline, glycerophosphocholine, histidine-betaine, *Nε*,*Nε*,*Nε*-trimethyllysine, *N*,*N*,*N*-trimethyltaurine, and proline-betaine. Measurement of ^{13}C chemical shifts using the ^{1}H−^{13}C heteronuclear single quantum coherence (HSQC) experiment at 700 MHz was valuable in the validation of resonance assignments (Table S-1), as demonstrated in the $N(CH_3)_3$ region (Figure S-3B) in which the ^{1}H−^{13}C chemical shift pairs helped reaffirm resonant assignment of betaine analogs.[24−27] With these several layers of metabolite confirmation, compounds identified by NMR are well-vetted, thus providing high levels of confidence.

Comparison of the CF, CC, and Tissue Metabolomes

Thirty-three common metabolites were observed in CF, CC, and tissue extracts, mostly consisting of sugars, organic acids, and amino acids (Table 1). 2-Aminobutyrate, asparagine, cytosine, histidine, 3-hydroxybutyrate, phenylalanine, propionate, and uridine were only detected in the CF and tissue, while ADP, AMP, and ATP were only found in the CC and tissue extracts. ATP was previously reported in CF but was not detected in our samples.[12] A major component of the coelom metabolome is TCA cycle constituents and their perturbation can give insights into bioenergetic stress. The ^{1}H NMR spectra of tissue extracts also contain the resonances of many of these constituents, although small changes in the levels of these metabolites may be more difficult to discern. Tissue extracts contain mostly amino acids, while, except for alanine, they tend to be minor components of the coelom.

Recently, Liebeke et al. unlocked a key defense required for biogeochemical cycling: dialkylfuransulfonate (termed drilodefensin) metabolites, which protect earthworms from the multitude of plant polyphenols to which they are exposed through their diet.[31] Tissue extracts contain a substantial concentration of the drilodefensin 2-hexyl-5-ethyl-furan-3-sulfonate (HEFS) (Figure 1), which is not observed within the coelom, in addition to glycerol, lysine, mannose, nicotinamide, nicotinate, nicotinurate, and trigonelline (Table 1 and Table S-1).

The high degree of similarity between the ^{1}H NMR spectra measured for CC and CF indicates that there is a close interaction between the two compartments. As observed in Figure 1, the lower intensity of the sugar resonances in the coelomocytes reveals additional resonances from *myo*-inositol, *Nε*,*Nε*,*Nε*-trimethyllysine (TML), and riboflavin. The resonances of glutamine and glutamate are also less overlapped with other signals in the coelomocyte spectra. Metabolite investigations in CF, CC, and tissue provide complementary and unique insights into earthworm metabolism.

Identification of a New Metabolite: Malylglutamate

Malylglutamate or 2-(3-carboxy-2-hydroxypropanamido)-pentanedioic acid is a previously unreported metabolite elucidated in these studies using NMR and high-resolution mass spectrometry (HRMS). Two sets of unassigned resonances (Figure 2A), denoted as 1H (green) and 2H (blue), were consistently observed in all matrices. The resonance at 2.23 ppm (2H*γ*; Figure 2A) was initially noted for its uncanny similarity in terms of coupling and intensity to that produced by the H*γ* of the free amino acid glutamate

DOI: 10.1021/acs.jproteome.7b00439
J. Proteome Res. 2017, 16, 3407−3418

(Figure 2A), suggesting the possibility of a glutamate (Glu) analog. The Glu-like 2H spin system was revealed in the TOCSY spectrum (Figure 2B), further supporting the hypothesis. Through comparison of numerous CF and CC spectra, we noticed a correlation in the intensity of the 2H and 1H resonances (Figure S-4), which we initially hypothesized could arise from an aspartyl moiety as a dipeptide due to its shared ABX coupling pattern.

To investigate the presence of a dipeptide, we measured the TOCSY spectrum of a concentrated CF sample in 90% H_2O at pD 3.18, revealing a strong correlation between an amide proton and a spin system resembling glutamate (Figure 2C) further supporting the assignment to a dipeptide. Several dipeptides were obtained, and their ^{1}H NMR spectra were recorded under conditions similar to those of the CF and CC extracts. Glutamylaspartate (Glu-Asp) produced similar chemical shifts for the aspartyl moiety but notably different chemical shift and *J*-coupling pattern for the GluHγ resonance, which collapsed to a triplet (Figure 2A) and is consistently observed in aspartylglutamate (Asp-Glu) and *N*-acetylaspartylglutamate (NAAG). The GluHγ of Asp-Glu and NAAG is shifted upfield to Glu (Figure 2A) like the unassigned 2Hγ, unlike the GluHγ of Glu-Asp, which is shifted downfield. On the basis of this result, we surmised that the glutamate group must be present at the dipeptide C-terminus, and indeed the Asp-Glu and NAAG coupling patterns, besides GluHγ, produced similar resonances to those observed in our CF and CC spectra (Figure 2A). Because of the lack of correspondence of the Asp chemical shifts of these dipeptides with the unassigned 1HABX resonances (Figure 2A), we were forced to consider other alternatives.

We proceeded to consider the similarity of the unassigned ABX resonances with malate, as annotated in Figure 2A,B, suggesting that the dipeptide could be malylglutamate (Mal-Glu). Supporting this hypothesis, the ^{1}H and ^{13}C chemical shifts and 2Hγ *J*-coupling of our unknown closely resembled that of β-citrylglutamate, described in Collard et al.[32] We were unable to identify reference to Mal-Glu in the literature or to locate a commercial source of the compound for verification by NMR. Therefore, we turned to HRMS to explore our hypothesis that the unknown metabolite could be Mal-Glu.

A diluted CF sample was directly infused into the mass spectrometer (DI–MS), yielding the Mal-Glu parent ion at *m/z* 264.0667 (the calculated *m/z* 264.0719 for the $[M + H]^+$ ion; Figure 3A). Ions in the MS/MS (Figure 3B) of the $[M + H]^+$ ion were assigned: *m/z* 246.1 $[M - H_2O]^+$; 227.9 $[M - 2H_2O]^+$; 220.1 $[M - CO_2]^+$; 190.0 $[M - CH_3CH_3COOH]^+$; and 146.0 $[M - CHOCH(OH)CH_2COOH]^+$. The fragments at *m/z* 146.0, 190.0, and 220.1 show the loss of three distinct groups around the single central nitrogen, confirming the presence of the amide bond and C-terminus of the Glu residue. The peak at *m/z* 232.1 is thought to arise from a cofragmenting species with the same *m/z* value as the newly discovered analyte due to the nature of the complex matrix of CF. Taken together, the NMR and HRMS results provide a high level of confidence that the unknown metabolite is Mal-Glu, first reported herein.

Identification of *Nδ,Nδ,Nδ*-Trimethylornithine—A New Metabolite in CF

Nδ,Nδ,Nδ-Trimethylornithine or TMO (3.129 ppm) (CAS: 66101-16-4) was identified as the neighboring singlet to *Nε,Nε,Nε*-trimethyllysine or TML (3.108 ppm), as shown in

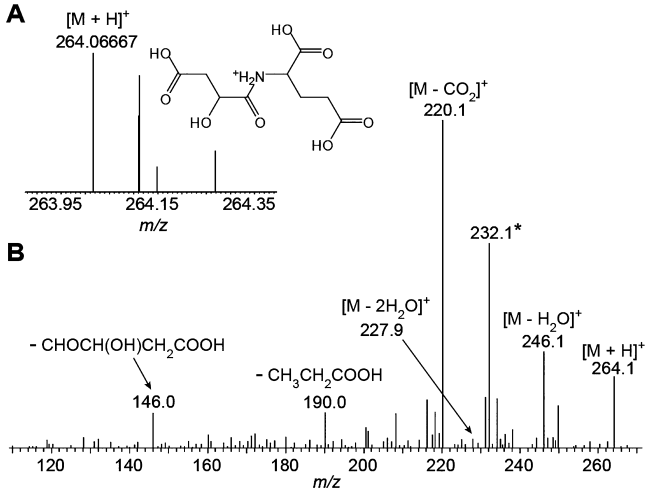

Figure 3. Confirmation of malylglutamate in a diluted CF sample using positive-ion ESI–MS and MS/MS. (A) Positive-ion ESI–MS of malylglutamate (the calculated *m/z* 264.0719 for $[M + H]^+$ ion) with its structure and (B) annotated MS/MS for the $[M + H]^+$ ion of malylglutamate. * indicates a peak from an ion cofragmenting with the $[M + H]^+$ ion.

Figure 4A, using a combination of NMR and HRMS. In the CF pH titration experiments, the chemical shifts of $N(CH_3)_3$ groups were affected minimally with increasing acidity (Figure S-1A), demonstrating that the singlets belonged to non-titratable groups. A weak cation exchange (WCX) solid-phase extraction strategy was employed simplify the mixture but did not offer any additional NMR insights due to the high chemical shift similarity of $N(CH_3)_3$ groups (Figure S-5A). To aid identification, the WCX eluate was subjected to LC–MS, allowing detection of the TMO parent ion at *m/z* 175.1431 (the calculated *m/z* 175.1447 for M^+ ion; Figure 4B). Figure 4C illustrates the MS/MS of the M^+ ion, yielding major fragments at *m/z* 116.1 $[M - N(CH_3)_3]^+$ and 60.1 $[HN(CH_3)_3]^+$ and minor fragment ions at *m/z* 157.0 $[M - H_2O]^+$, 147.1 $[M - CO]^+$; 133.1 $[M - CO_2]^+$; and 130.1 $[M - HN(CH_3)_2]^+$. In this context, the loss of dimethylamine (i.e., $HN(CH_3)_2$) may be initiated from the migration of a methyl group from the trimethylammoium moiety, and such migration was previously observed for singly charged peptides harboring a trimethyllysine.[33] The fragmentation of TMO, TML, and betaine (Figure S-5B–E), is consistent with reported fragmentation of betaine analogs.[34]

TMO's N$\delta(CH_3)_3$ chemical shift is downfield of TML, consistent with the additional CH_2 group of TML. Also, the resonance is consistent with the reported N$\delta(CH_3)_3$ shift of ornithine betaine, which has ornithine trimethylated on both amines.[35] The other TMO resonances are observed in our TOCSY spectra (Figure 4D) at similar chemical shifts to TMO, as described in Patti et al.[36] Finally, the TMO/TML ratios were approximately 1:5 and 1:3, respectively, in HRMS and NMR. It is expected that these ratios are not identical due to differences in ionization, resolution, and sample preparation; however, the similarity of the two ratios obtained with orthogonal analytical platforms further supports the assignment of TMO as the unknown.

Other Newly Identified Metabolites in CF, CC, and Tissue

2-Aminobutyrate in the CF and nicotinurate and trigonelline in tissue extracts were also newly detected metabolites using 1D

DOI: 10.1021/acs.jproteome.7b00439
J. Proteome Res. 2017, 16, 3407–3418

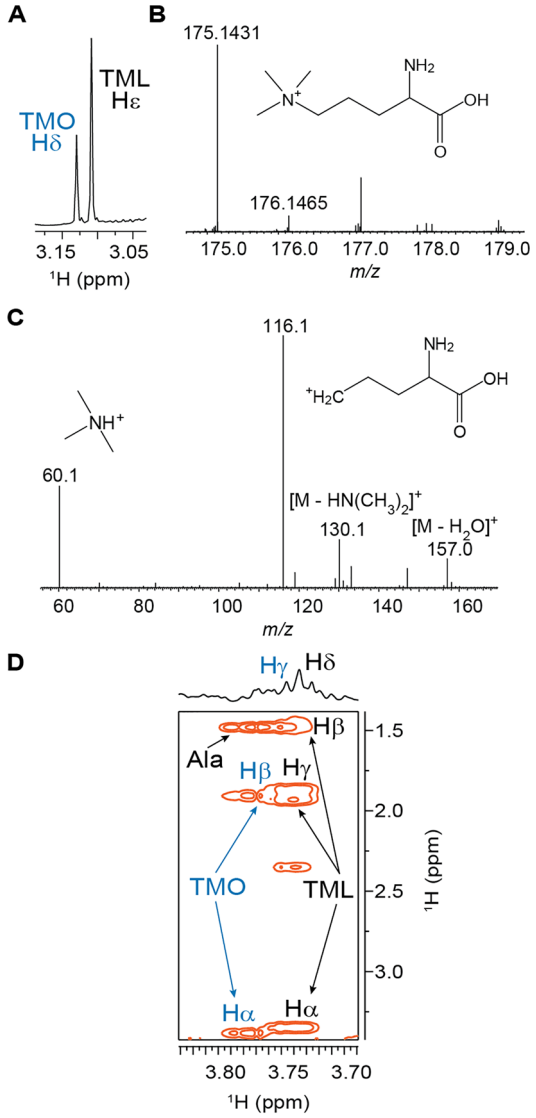

Figure 4. LC–MS identification of TMO and NMR confirmation. (A) $N(CH_3)_3$ singlets of TML and TMO between 3.05 and 3.15 ppm. (B) Positive-ion ESI–MS of TMO (the calculated m/z 175.1447 for the M^+ ion); shown are the monoisotopic peak at m/z 175.1431 and the structure of TMO. (C) MS/MS for the M^+ ion of TMO and (D) CF TOCSY spectrum with labeled TMO and TML spin systems. The TMO Nδ $(CH_3)_3$ and TML N$\varepsilon(CH_3)_3$ singlets are not correlated with these spin systems because the carbon-bound protons on either side of the nitrogen are too distant to be coupled to one another. Overlapped resonances of TML and alanine (Ala) are annotated to emphasize that the peak does not belong to the TMO spin system.

and 2D NMR spectra and by comparison with authentic standards (Figure S-6). Previously maltose has been reported within earthworms, but here we report the resonances as maltose-x due to the several overlapping resonances of maltose, maltotriose, and potentially other closely related sugars.

Rochfort et al. recently described an *E. fetida* and *E. andrei* specific aromatic metabolites that we suspect may correlate with resonances in our CF NMR spectra and peaks detected in our DI–MS experiments, but because of the limited HRMS and NMR data reported and commercially unavailable standards, we could not confidently assign the ion or similar resonances as the reported metabolites.[37] Earthworms contain an abundance of unique metabolites, and further elucidation of new metabolites and probing of their biochemical function could aid environmental monitoring and diagnostics.

DISCUSSION

In this work, the complex and metabolite-rich *E. fetida* CF, CC, and tissue metabolomes were characterized using NMR spectroscopy. The abundance of TCA metabolites, osmolytes, polyamines, and other metabolites detected in these studies indicates that the CF may serve as a metabolic reservoir. Our elucidation of the coelomocyte metabolome offers a new source to evaluate earthworm health and possible insights into hepatocytic and immune function, while tissue extracts offer a metabolic summary of global processes occurring within the earthworm. These studies newly detected 2-aminobutyrate, nicotinurate, *Nδ,Nδ,Nδ*-trimethylornithine, and trigonelline and, notably, elucidated a new compound: malylglutamate.

Possible Biochemical Significance of Malylglutamate

Malylglutamate is structurally analogous to *β*-citrylglutamate and NAAG (Figure 5), and we hypothesize that its synthesis

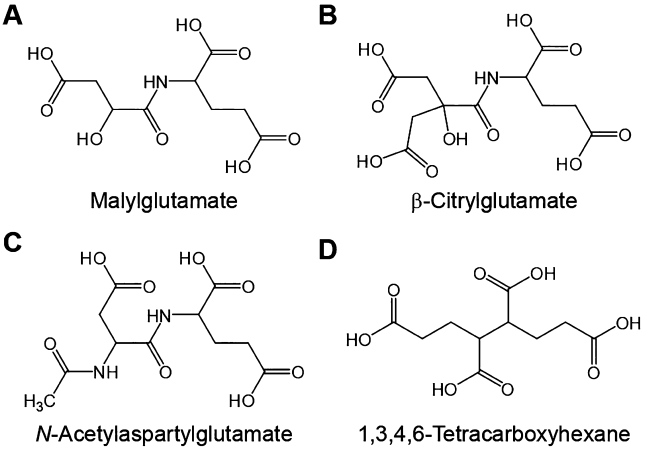

Figure 5. Chemical structures of (A) malylglutamate, (B) *β*-citrylglutamate, (C) *N*-acetylaspartylglutamate (NAAG), and (D) 1,3,4,6-tetracarboxyhexane.

and hydrolysis occurs via parallel pathways. NAAG and *β*-citrylglutamate are synthesized by homologous ligases to *Escherichia coli* RIMKLA and RIMKLB, respectively.[32] Whereas citrate is not a suitable substrate for RIMKLA, RIMKLB can ligate *N*-acetylaspartate and glutamate at similar rates to citrate and glutamate. The authors were not surprised by this finding because citrate and *N*-acetylaspartate are nearly isosteric. This suggests that RIMKLB is less specific than RIMKLA, and it is feasible that the structurally similar malate could be a suitable substrate in an environment or system with higher malate levels compared with citrate, as is the case with *E. fetida* CF. *β*-Citrylglutamate is cleaved into citrate and glutamate by *β*-citrylglutamate hydroxylase (i.e., glutamate carboxypeptidase 3), a glycosylated, membrane-bound ectoenzyme that is active only extracellularly.[38] Malate levels are strikingly higher in the CF compared with the CC (Figure 1 and Figure S-4), suggesting that malylglutamate hydrolysis may occur by this or a related ectoenzyme in the coelomic cavity, presumably to feed the TCA cycle and provide energy to muscle and CC.

Malylglutamate plausibly serves as a TCA cycle store that can be hydrolyzed to malate and glutamate when energy demand increases. Malylglutamate is also homologous to the anionic

DOI: 10.1021/acs.jproteome.7b00439
J. Proteome Res. 2017, 16, 3407–3418

osmolyte 1,3,4,6-tetracarboxyhexane (Figure 5D), found in archaea, that helps counter K^+ concentrations under osmotic stress.[39] Malylglutamate is found in approximately a 1:1 ratio with TMO and TML (i.e., Mal-Glu:(TMO+TML)), suggesting that malylglutamate assists homeostasis by maintaining charge balance with the cationic betaine analogs, in addition to acting as an anionic osmolyte to aid varying soil moisture contents. Lastly, we hypothesize that malylglutamate is a chelator, like β-citrylglutamate which can sequester iron and copper.[40,41] β-Citrylglutamate may act as a chaperone for iron to aconitase and protective complex against NO-induced aconitase inhibition.[42,43] Malylglutamate may form similar complexes to aid biochemical processes or protect the worm against metal burdens. The physiological functions of malylglutamate need further exploration to understand its unique presence and abundance in earthworms.

Betaine Analogs and Osmoregulation

As the cationic counterpart to malylglutamate, earthworms contain an arsenal of betaine analogs, including: betaine, choline, glycerophosphocholine, histidine-betaine, *N*,*N*-dimethylhistidine, *N*,*N*,*N*-trimethyltaurine, TML, and TMO. Proline-betaine was only detected in tissue samples, while γ-butyrobetaine was only detected in the CC and CF. Liebeke and Bundy reported γ-butyrobetaine in the $^{1}H-^{13}C$ HSQC spectra measured at 800 MHz of *E. fetida* whole-worm extracts, potentially due to increased sensitivity compared with our measured HSQC data at 700 MHz. The authors also detected carnitine and hydroxyproline-betaine in the whole-worm extracts of other earthworm species, but these were not detected in our NMR spectra.

The function of betaine analogs is unclear, but it is hypothesized that they may serve as osmoprotective agents for proteins and membranes. Earthworms must constantly adjust to changing moisture content in soil, and CF contains many other well known osmolytes like betaine, glucose, inositol, trehalose, and polyamines. For instance, upregulation of glucose and alanine was observed in *Enchytraeus albidus* under drought conditions, while only alanine level increased in *A. caliginosa* in response to estivation.[44,45] Future studies should explore the role of betaines under similar contexts and aim to establish the biochemical functions of this diverse group of earthworm metabolites.

It should also be noted that TML, γ-butyrobetaine, α-ketoglutarate, and succinate are a part of the carnitine biosynthesis pathway, which is essential for converting fatty acids into energy via mitochondrial and peroxisomal β-oxidation. TMO was recently revealed as a suitable substrate for TML hydroxylase, converting 75% of TMO to 3-hydroxy-*Nδ*,*Nδ*,*Nδ*-trimethylornithine.[46] This may suggest that TMO and other betaine analogs may act as an alternative substrate when TML is limited. In mammals, the liver is the central location of the final conversion of γ-butyrobetaine by γ-butyrobetaine dioxygenase to carnitine.[47] Because γ-butyrobetaine is only observed in the coelom and some subsets of coelomocytes serve liver-like functions, this may explain the presence of γ-butyrobetaine in CC extracts.

Polyamines

E. fetida also contains a significant quantity of polyamines (putrescine, spermidine, and spermine) within its CC and CF. Polyamines are fully protonated under physiological conditions, consistent with their various functions, which include moderating ion channels, cell growth and differentiation, gene expression, apoptosis, and chromatin status.[48] Disruption of polyamine synthesis, indicated by their downregulation, has been suggested as a sign of genotoxicity, while their upregulation acts as a protective response against oxidative, osmotic, and thermal stress. Consistently observed in *E. fetida*, organisms that are able to regenerate have a close association with polyamine metabolism and synthesis.[49] Putrescine was upregulated in response to removal and regeneration of worm heads. In the same study, osmotic and heat shock temporarily upregulated putrescine and spermidine. Elevation in putrescine was additionally observed in *L. rubellus* exposed to high levels of nickel.[50] Similarly, upregulation of putrescine and alanine in two *A. caliginosa* populations exposed to the fungicide epoxyiconazole was credited as a stress indicator.[51] Moreover, endosulfan and endosulfan sulfate exposure were hypothesized to induce genotoxicity that resulted in apoptosis and thus subsequently decreased spermidine concentrations within *E. fetida* CF.[12,13] This suggests that the CF may act as a reservoir for polyamines, and probing their alteration may prove to be a useful indicator of environmental stress.

Coelomocytes

Giving its characteristic bright-yellow hue, riboflavin is found at substantial concentrations within the CC and CF. Riboflavin stored in CC has been identified as a coelomocyte chemoattractant in six earthworm species and may serve as a recruiting factor to combat microbial invasion.[52,53] Interestingly, riboflavin content in CC has been explored as an indicator of heavy metal toxicity and soil health. Plytycz et al. hypothesized that the heavy metal body burden is localized in the chloragogenous tissue of the worm, a source of a type of CC called elocytes, explaining how heavy metal exposure interferes with worm's immune response.[54] In this study, stimulation of the immune system by chronic heavy metal exposure led to riboflavin depletion in the CC of *Dendrodrilus rubidus*, marking the potential of riboflavin in elocytes as an indicator of heavy metal toxicity. These studies highlight the potential of riboflavin and coelomocytes as a tool to indicate metal contamination.

CONCLUSIONS

From drilodefensins to betaine analogs to malylglutamate, earthworms are equipped with an abundance of unique metabolites. Still, unassigned resonances remain in earthworm NMR spectra, particularly in the aromatic region where conjugation and proton position on the aromatic ring result in complex *J*-coupling patterns, whose coupling is difficult to distinguish in complex mixtures. Separation techniques to target aromatic compounds can be employed to simplify spectra, but due to resonance overlap, other analytical techniques like mass spectrometry may be more useful to identify aromatic unknowns. Performing measurements at higher magnetic fields improves both spectral resolution and sensitivity and may be useful in the identification of minor species. Complexity due to resonance overlap can also be overcome through isotopic labeling of specific functional groups; for example, ^{13}C-formlyation of amines and ^{15}N-ethanolamine tagging of carboxylates have improved the sensitivity and resolution of metabolite assignments using 2D NMR experiments.[55,56] Less resonance overlap is observed in ^{13}C and ^{15}N NMR compared with ^{1}H NMR, and recent advancements in dissolution dynamic nuclear polarization have improved ^{13}C sensitivity, thus increasing the feasibility of using 1D ^{13}C experiments in metabolic profiling.[57] Other tactics used

DOI: 10.1021/acs.jproteome.7b00439
J. Proteome Res. 2017, 16, 3407−3418

identify metabolites include chemical separation or orthogonal analytical techniques like Fourier transform-infrared spectroscopy or mass spectrometry.

Mass spectrometry has remained sparse in earthworm metabolomic research , but could offer insights into additional biochemical pathways and new metabolites. Gas chromatography−mass spectrometry (GC−MS) is commonly used in untargeted metabolic profiling experiments.[58] It been employed to probe metabolic perturbations by xenobiotics in whole-worm extracts, revealing insights into fatty acids, low-level amino acids, carbohydrates, and lipids not detected in ^{1}H NMR spectra, yet GC−MS analysis of CF and CC extracts remains unreported.[50,59−63] LC−MS has been used to aid metabolite elucidation, but surprisingly targeted and untargeted LC−MS approaches remain unused to probe the earthworm metabolome. Targeted LC−MS can be used to survey chemical classes or biochemical pathways, like phosphorylated sugars, aiding metabolite elucidation or insights into specific metabolic functions.[64] Extending the use of MS in earthworm metabolomics can help elucidate unassigned resonances in the ^{1}H NMR spectra and give new insights into the biochemical function of unique earthworm metabolites.

As demonstrated in this study, NMR offers a means to quantify a diverse range of metabolites within earthworms for systems toxicology research or environmental monitoring. Ultimately, this study resulted in the elucidation of a new metabolite: Malylglutamate, which we hypothesize acts as an anionic osmolyte, helps maintain electrolyte balance within CF and cells, is a metal ion chelator, and serves as a malate/glutamate reservoir. Our work, and that of similar studies, provides a platform to enhance the understanding of earthworm metabolism and illustrates the potential for high-throughput NMR analysis to deliver a quick snapshot of earthworm, soil, and ecological health.

■ ASSOCIATED CONTENT

Supporting Information

The Supporting Information is available free of charge on the ACS Publications website at DOI: 10.1021/acs.jproteome.7b00439.

Table S-1. ^{13}C chemical shifts of detected metabolites using ^{1}H−^{13}C HSQC spectroscopy. Figure S-1. ^{1}H NMR spectra of CF pH titration. Figure S-2. Representative COSY spectrum. Figure S-3. Representative spectra of metabolite assignments using homonuclear 2D *J*-resolved spectroscopy and ^{1}H−^{13}C HSQC spectroscopy. Figure S-4. Depiction of unassigned resonances. Figure S-5. Weak cation exchange separation of cationic metabolites in CF and LC−MS identification of betaine and *Nε*,*Nε*,*Nε*-trimethyllysine. Figure S-6. Depiction 2-aminobutyrate, nicotinurate, and trigonelline ^{1}NMR assignments. (PDF)

■ AUTHOR INFORMATION

Corresponding Author

*E-mail: clarive@ucr.edu. Tel: 951-827-2990. Fax: 951-827-2435.

ORCID

Corey M. Griffith: 0000-0001-9104-9501
Yinsheng Wang: 0000-0001-5565-283X
Cynthia K. Larive: 0000-0003-3458-0771

Author Contributions

C.M.G and C.K.L. designed the experiments and wrote the manuscript. P.B.W. conducted the mass spectrometry experiments and data interpretation under the guidance of Y.W. L.W.T and M.M.D. aided with NMR acquisition and data interpretation.

Notes

The authors declare no competing financial interest.

■ ACKNOWLEDGMENTS

We thank Alvicler Magalhaes for his helpful discussions to this work; Dan Borchardt and the Analytical Chemistry Instrument Facility (ACIF) at the University of California, Riverside for use of their 700 MHz NMR; and Hugo Campos for his benchwork assistance. C.M.G. acknowledges support from the National Institutes of Health training grant T32 ES018827; L.W.T. acknowledges support from the Coordenação de Aperfeiçoamento de Pessoal de Nível Superior - CAPES Estágio Sênior grant 99999.006402/2014-03; and Y.W. acknowledges support from the National Institutes of Health grant P01AG043376.

■ ABBREVIATIONS

Asp-Glu, aspartylglutamate; CC, coelomocytes; CF, coelomic fluid; COSY, correlation spectroscopy; DI−MS, direct infusion−mass spectrometry; GC−MS, gas chromatography−mass spectrometry; Glu-Asp, glutamylaspartate; HEFS, 2-hexyl-5-ethyl-furan-3-sulfonate; HRMS, high-resolution mass spectrometry; HSQC, heteronuclear single quantum correlation spectroscopy; LC−MS, liquid chromatography−mass spectrometry; NAAG, *N*-acetylaspartylglutamate; Mal-Glu, malylglutamate; NMR, nuclear magnetic resonance; OECD, organization for economic cooperation and development; TCA, tricarboxylic acid cycle; TFA, trifluoroacetic acid; TML, *Nε*,*Nε*,*Nε*-trimethyllysine; TMO, *Nδ*,*Nδ*,*Nδ*-trimethylornithine; TOCSY, total correlation spectroscopy; WCX, weak cation exchange

■ REFERENCES

(1) Lankadurai, B. P.; Nagato, E. G.; Simpson, M. J. Environmental metabolomics: An emerging approach to study organism responses to environmental stressors. *Environ. Rev.* **2013**, *21* (3), 180−205.

(2) Brulle, F.; Morgan, A. J.; Cocquerelle, C.; Vandenbulcke, F. Transcriptomic underpinning of toxicant-mediated physiological function alterations in three terrestrial invertebrate taxa: A review. *Environ. Pollut.* **2010**, *158* (9), 2793−2808.

(3) Ji, C. L.; Wu, H. F.; Wei, L.; Zhao, J. M.; Lu, H. J.; Yu, J. B. Proteomic and metabolomic analysis of earthworm eisenia fetida exposed to different concentrations of 2,2 ′,4,4 ′-tetrabromodiphenyl ether. *J. Proteomics* **2013**, *91*, 405−416.

(4) Bundy, J.; Sidhu, J.; Rana, F.; Spurgeon, D.; Svendsen, C.; Wren, J.; Sturzenbaum, S.; Morgan, A. J.; Kille, P. 'Systems toxicology' approach identifies coordinated metabolic responses to copper in a terrestrial non-model invertebrate, the earthworm lumbricus rubellus. *BMC Biol.* **2008**, *6* (1), 25.

(5) Edwards, C. A.; Bohlen, P. J. *Biology and Ecology of Earthworms*, 3rd ed.; Chapman & Hall: London, U.K., 1996; pp 11−12.

(6) Bilej, M.; Procházková, P.; Šilerová, M.; Josková, R. Earthworm Immunity. In *Invertebrate Immunity*; Söderhäll, K., Ed.; Springer: 2010; Vol. *708*, pp 66−79.

(7) Bundy, J. G.; Osborn, D.; Weeks, J. M.; Lindon, J. C.; Nicholson, J. K. An nmr-based metabonomic approach to the investigation of coelomic fluid biochemistry in earthworms under toxic stress. *FEBS Lett.* **2001**, *500* (1−2), 31−35.

DOI: 10.1021/acs.jproteome.7b00439
J. Proteome Res. 2017, 16, 3407−3418

(8) Burch, W. S.; Fitzpatrick, C. L.; Goven, J. A.; Venables, J. B.; Giggleman, A. M. In vitro earthworm lumbricus terrestris coelomocyte assay for use in terrestrial toxicity identification evaluation. *Bull. Environ. Contam. Toxicol.* **1999**, *62* (5), 547−554.
(9) Klobucar, G. I. V.; Stambuk, A.; Srut, M.; Husnjak, I.; Merkas, M.; Traven, L.; Cvetkovic, Z. Aporrectodea caliginosa, a suitable earthworm species for field based genotoxicity assessment? *Environ. Pollut.* **2011**, *159* (4), 841−849.
(10) Griffith, C. M.; Baig, N.; Seiber, J. N. Contamination from Industrial Toxicants. In *Handbook of Food Chemistry*; Cheung, P. C. K., Mehta, B. M., Eds.; Springer: Berlin, 2015; pp 719−751.
(11) Griffith, C. M.; Woodrow, J. E.; Seiber, J. N. Environmental behavior and analysis of agricultural sulfur. *Pest Manage. Sci.* **2015**, *71* (11), 1486−1496.
(12) Yuk, J.; Simpson, M. J.; Simpson, A. J. Coelomic fluid: A complimentary biological medium to assess sub-lethal endosulfan exposure using h-1 nmr-based earthworm metabolomics. *Ecotoxicology* **2012**, *21* (5), 1301−1313.
(13) Yuk, J.; Simpson, M. J.; Simpson, A. J. 1-d and 2-d nmr-based metabolomics of earthworms exposed to endosulfan and endosulfan sulfate in soil. *Environ. Pollut.* **2013**, *175*, 35−44.
(14) Bundy, J. G.; Spurgeon, D.; Svendsen, C.; Hankard, P.; Osborn, D.; Lindon, J.; Nicholson, J. Earthworm species of the genus eisenia can be phenotypically differentiated by metabolic profiling. *FEBS Lett.* **2002**, *521*, 115−120.
(15) Larive, C. K.; Barding, G. A.; Dinges, M. M. Nmr spectroscopy for metabolomics and metabolic profiling. *Anal. Chem.* **2015**, *87* (1), 133−146.
(16) Nagana Gowda, G. A.; Raftery, D. Recent advances in nmr-based metabolomics. *Anal. Chem.* **2017**, *89* (1), 490−510.
(17) Giraudeau, P. Challenges and perspectives in quantitative nmr. *Magn. Reson. Chem.* **2017**, *55* (1), 61−69.
(18) Brown, S. A. E.; Simpson, A. J.; Simpson, M. J. Evaluation of sample preparation methods for nuclear magnetic resonance metabolic profiling studies with eisenia fetida. *Environ. Toxicol. Chem.* **2008**, *27* (4), 828−836.
(19) Bax, A.; Davis, D. G. Mlev-17-based two-dimensional homonuclear magnetization transfer spectroscopy. *J. Magn. Reson.* **1985**, *65* (2), 355−360.
(20) Liu, M.; Mao, X.-a.; Ye, C.; Huang, H.; Nicholson, J. K.; Lindon, J. C. Improved watergate pulse sequences for solvent suppression in nmr spectroscopy. *J. Magn. Reson.* **1998**, *132* (1), 125−129.
(21) Davis, A. L.; Laue, E. D.; Keeler, J.; Moskau, D.; Lohman, J. Absorption-mode two-dimensional nmr spectra recorded using pulsed field gradients. *J. Magn. Reson.* **1991**, *94* (3), 637−644.
(22) Piantini, U.; Sorensen, O. W.; Ernst, R. R. Multiple quantum filters for elucidating nmr coupling networks. *J. Am. Chem. Soc.* **1982**, *104* (24), 6800−6801.
(23) Aue, W. P.; Karhan, J.; Ernst, R. R. Homonuclear broad band decoupling and two-dimensional j-resolved nmr spectroscopy. *J. Chem. Phys.* **1976**, *64* (10), 4226−4227.
(24) Palmer, A. G.; Cavanagh, J.; Wright, P. E.; Rance, M. Sensitivity improvement in proton-detected two-dimensional heteronuclear correlation nmr spectroscopy. *J. Magn. Reson.* **1991**, *93* (1), 151−170.
(25) Kay, L.; Keifer, P.; Saarinen, T. Pure absorption gradient enhanced heteronuclear single quantum correlation spectroscopy with improved sensitivity. *J. Am. Chem. Soc.* **1992**, *114* (26), 10663−10665.
(26) Willker, W.; Leibfritz, D.; Kerssebaum, R.; Bermel, W. Gradient selection in inverse heteronuclear correlation spectroscopy. *Magn. Reson. Chem.* **1993**, *31* (3), 287−292.
(27) Schleucher, J.; Schwendinger, M.; Sattler, M.; Schmidt, P.; Schedletzky, O.; Glaser, S. J.; Sørensen, O. W.; Griesinger, C. A general enhancement scheme in heteronuclear multidimensional nmr employing pulsed field gradients. *J. Biomol. NMR* **1994**, *4* (2), 301−306.
(28) Cui, Q.; Lewis, I. A.; Hegeman, A. D.; Anderson, M. E.; Li, J.; Schulte, C. F.; Westler, W. M.; Eghbalnia, H. R.; Sussman, M. R.; Markley, J. L. Metabolite identification via the madison metabolomics consortium database. *Nat. Biotechnol.* **2008**, *26* (2), 162−164.
(29) Wishart, D. S.; Jewison, T.; Guo, A. C.; Wilson, M.; Knox, C.; Liu, Y.; Djoumbou, Y.; Mandal, R.; Aziat, F.; Dong, E.; Bouatra, S.; Sinelnikov, I.; Arndt, D.; Xia, J.; Liu, P.; Yallou, F.; Bjorndahl, T.; Perez-Pineiro, R.; Eisner, R.; Allen, F.; Neveu, V.; Greiner, R.; Scalbert, A. Hmdb 3.0—the human metabolome database in 2013. *Nucleic Acids Res.* **2013**, *41* (D1), D801−D807.
(30) Madalinski, G.; Godat, E.; Alves, S.; Lesage, D.; Genin, E.; Levi, P.; Labarre, J.; Tabet, J.-C.; Ezan, E.; Junot, C. Direct introduction of biological samples into a ltq-orbitrap hybrid mass spectrometer as a tool for fast metabolome analysis. *Anal. Chem.* **2008**, *80* (9), 3291−3303.
(31) Liebeke, M.; Strittmatter, N.; Fearn, S.; Morgan, A. J.; Kille, P.; Fuchser, J.; Wallis, D.; Palchykov, V.; Robertson, J.; Lahive, E.; Spurgeon, D. J.; McPhail, D.; Takats, Z.; Bundy, J. G. Unique metabolites protect earthworms against plant polyphenols. *Nat. Commun.* **2015**, *6*, 7869.
(32) Collard, F.; Stroobant, V.; Lamosa, P.; Kapanda, C. N.; Lambert, D. M.; Muccioli, G. G.; Poupaert, J. H.; Opperdoes, F.; Van Schaftingen, E. Molecular identification of n-acetylaspartylglutamate synthase and β-citrylglutamate synthase. *J. Biol. Chem.* **2010**, *285* (39), 29826−29833.
(33) Xiong, L.; Ping, L.; Yuan, B.; Wang, Y. Methyl group migration during the fragmentation of singly charged ions of trimethyllysine-containing peptides: Precaution of using ms/ms of singly charged ions for interrogating peptide methylation. *J. Am. Soc. Mass Spectrom.* **2009**, *20* (6), 1172−1181.
(34) Naresh Chary, V.; Dinesh Kumar, C.; Vairamani, M.; Prabhakar, S. Characterization of amino acid-derived betaines by electrospray ionization tandem mass spectrometry. *J. Mass Spectrom.* **2012**, *47* (1), 79−88.
(35) Liebeke, M.; Bundy, J. G. Biochemical diversity of betaines in earthworms. *Biochem. Biophys. Res. Commun.* **2013**, *430* (4), 1306−1311.
(36) Patti, A.; Morrone, R.; Chillemi, R.; Piattelli, M.; Sciuto, S. Biosynthetic relationships between sulfonium and n-methylated compounds in the red alga vidalia volubilis. *J. Nat. Prod.* **1992**, *55* (1), 53−57.
(37) Rochfort, S.; Wyatt, M. A.; Liebeke, M.; Southam, A. D.; Viant, M. R.; Bundy, J. G. Aromatic metabolites from the coelomic fluid of eisenia earthworm species. *Eur. J. Soil Biol.* **2017**, *78*, 17−19.
(38) Collard, F.; Vertommen, D.; Constantinescu, S.; Buts, L.; Van Schaftingen, E. Molecular identification of beta-citrylglutamate hydrolase as glutamate carboxypeptidase 3. *J. Biol. Chem.* **2011**, *286* (44), 38220−38230.
(39) Ciulla, R.; Clougherty, C.; Belay, N.; Krishnan, S.; Zhou, C.; Byrd, D.; Roberts, M. F. Halotolerance of methanobacterium thermoautotrophicum delta h and marburg. *J. Bacteriol.* **1994**, *176* (11), 3177−3187.
(40) Hamada-Kanazawa, M.; Kouda, M.; Odani, A.; Matsuyama, K.; Kanazawa, K.; Hasegawa, T.; Narahara, M.; Miyake, M. Beta-citryl-l-glutamate is an endogenous iron chelator that occurs naturally in the developing brain. *Biol. Pharm. Bull.* **2010**, *33* (5), 729−737.
(41) Narahara, M.; Hamada-Kanazawa, M.; Kouda, M.; Odani, A.; Miyake, M. Superoxide scavenging and xanthine oxidase inhibiting activities of copper s-citryl-l-glutamate complex. *Biol. Pharm. Bull.* **2010**, *33* (12), 1938−1943.
(42) Hamada-Kanazawa, M.; Narahara, M.; Takano, M.; Min, K. S.; Tanaka, K.; Miyake, M. Beta-citryl-l-glutamate acts as an iron carrier to activate aconitase activity. *Biol. Pharm. Bull.* **2011**, *34* (9), 1455−1464.
(43) Hamada-Kanazawa, M.; Narahara, M.; Takano, M.; Min, K. S.; Tanaka, K.; Miyake, M. Nitric oxide promotes survival of cerebral cortex neurons with simultaneous addition of fe(ii)(beta-citryl-l-glutamate) complex in primary culture. *Biol. Pharm. Bull.* **2013**, *36* (7), 1068−1079.
(44) Maraldo, K.; Ravn, H.; Slotsbo, S.; Holmstrup, M. Responses to acute and chronic desiccation stress in enchytraeus (oligochaeta: Enchytraeidae). *J. Comp. Physiol., B* **2009**, *179* (2), 113−123.
(45) Bayley, M.; Overgaard, J.; Hoj, A. S.; Malmendal, A.; Nielsen, N. C.; Holmstrup, M.; Wang, T. Metabolic changes during estivation in

DOI: 10.1021/acs.jproteome.7b00439
J. Proteome Res. 2017, 16, 3407−3418

the common earthworm aporrectodea caliginosa. *Physiol. Biochem. Zool.* **2010**, *83* (3), 541−550.
(46) Al Temimi, A. H. K.; Pieters, B. J. G. E.; Reddy, Y. V.; White, P. B.; Mecinovic, J. Substrate scope for trimethyllysine hydroxylase catalysis. *Chem. Commun.* **2016**, *52* (87), 12849−12852.
(47) Vaz, F. M.; Wanders, R. J. A. Carnitine biosynthesis in mammals. *Biochem. J.* **2002**, *361* (3), 417−429.
(48) Polticelli, F.; Salvi, D.; Mariottini, P.; Amendola, R.; Cervelli, M. Molecular evolution of the polyamine oxidase gene family in metazoa. *BMC Evol. Biol.* **2012**, *12* (1), 90.
(49) Hamana, K.; Hamana, H.; Shinozawa, T. Alterations in polyamine levels of nematode, earthworm, leech and planarian during regeneration, temperature and osmotic stresses. *Comp. Biochem. Physiol., Part B: Biochem. Mol. Biol.* **1995**, *111* (1), 91−97.
(50) Baylay, A. J.; Spurgeon, D. J.; Svendsen, C.; Griffin, J. L.; Swain, S.; Sturzenbaum, S.; Jones, O. A. H. A metabolomics based test of independent action and concentration addition using the earthworm lumbricus rubellus. *Ecotoxicology* **2012**, *21* (5), 1436−1447.
(51) Givaudan, N.; Wiegand, C.; Le Bot, B.; Renault, D.; Pallois, F.; Llopis, S.; Binet, F. Acclimation of earthworms to chemicals in anthropogenic landscapes, physiological mechanisms and soil ecological implications. *Soil Biol. Biochem.* **2014**, *73*, 49−58.
(52) Mazur, A. I.; Klimek, M.; Morgan, A. J.; Plytycz, B. Riboflavin storage in earthworm chloragocytes and chloragocyte-derived eleocytes and its putative role as chemoattractant for immunocompetent cells. *Pedobiologia* **2011**, *54*, S37−S42.
(53) Santocki, M.; Falniowski, A.; Plytycz, B. Restoration of experimentally depleted coelomocytes in juvenile and adult composting earthworms eisenia andrei e. Fetida and dendrobaena veneta. *Appl. Soil Ecol.* **2016**, *104*, 163−173.
(54) Plytycz, B.; Lis-Molenda, U.; Cygal, M.; Kielbasa, E.; Grebosz, A.; Duchnowski, M.; Andre, J.; Morgan, A. J. Riboflavin content of coelomocytes in earthworm (dendrodrilus rubidus) field populations as a molecular biomarker of soil metal pollution. *Environ. Pollut.* **2009**, *157* (11), 3042−3050.
(55) Ye, T.; Mo, H.; Shanaiah, N.; Gowda, G. A. N.; Zhang, S.; Raftery, D. Chemoselective 15n tag for sensitive and high-resolution nuclear magnetic resonance profiling of the carboxyl-containing metabolome. *Anal. Chem.* **2009**, *81* (12), 4882−4888.
(56) Ye, T.; Zhang, S.; Mo, H.; Tayyari, F.; Gowda, G. A. N.; Raftery, D. 13c-formylation for improved nuclear magnetic resonance profiling of amino metabolites in biofluids. *Anal. Chem.* **2010**, *82* (6), 2303−2309.
(57) Bornet, A.; Maucourt, M.; Deborde, C.; Jacob, D.; Milani, J.; Vuichoud, B.; Ji, X.; Dumez, J.-N.; Moing, A.; Bodenhausen, G.; Jannin, S.; Giraudeau, P. Highly repeatable dissolution dynamic nuclear polarization for heteronuclear nmr metabolomics. *Anal. Chem.* **2016**, *88* (12), 6179−6183.
(58) Barding, G. A.; Beni, S.; Fukao, T.; Bailey-Serres, J.; Larive, C. K. Comparison of gc-ms and nmr for metabolite profiling of rice subjected to submergence stress. *J. Proteome Res.* **2013**, *12* (2), 898−909.
(59) Jones, O. A. H.; Spurgeon, D. J.; Svendsen, C.; Griffin, J. L. A metabolomics based approach to assessing the toxicity of the polyaromatic hydrocarbon pyrene to the earthworm lumbricus rubellus. *Chemosphere* **2008**, *71* (3), 601−609.
(60) McKelvie, J. R.; Yuk, J.; Xu, Y. P.; Simpson, A. J.; Simpson, M. J. H-1 nmr and gc/ms metabolomics of earthworm responses to sub-lethal ddt and endosulfan exposure. *Metabolomics* **2009**, *5* (1), 84−94.
(61) Mudiam, M. K. R.; Ch, R.; Saxena, P. N. Gas chromatography-mass spectrometry based metabolomic approach for optimization and toxicity evaluation of earthworm sub-lethal responses to carbofuran. *PLoS One* **2013**, *8* (12), e81077.
(62) Gillis, J. D.; Price, G. W.; Prasher, S. Lethal and sub-lethal effects of triclosan toxicity to the earthworm eisenia fetida assessed through gc-ms metabolomics. *J. Hazard. Mater.* **2017**, *323*, 203−211.
(63) Ch, R.; Singh, A. K.; Pandey, P.; Saxena, P. N.; Reddy Mudiam, M. K. Identifying the metabolic perturbations in earthworm induced by cypermethrin using gas chromatography-mass spectrometry based metabolomics. *Sci. Rep.* **2015**, *5*, 15674.
(64) Mathon, C.; Barding, G. A., Jr; Larive, C. K. Separation of ten phosphorylated mono-and disaccharides using hilic and ion-pairing interactions. *Anal. Chim. Acta* **2017**, *972*, 102−110.

DOI: 10.1021/acs.jproteome.7b00439
J. Proteome Res. 2017, 16, 3407−3418